Identification and Characterization of *O*-Acetylpeptidoglycan Esterase: A Novel Enzyme Discovered in *Neisseria gonorrhoeae*†

Joel T. Weadge and Anthony J. Clarke*

Department of Molecular and Cellular Biology, University of Guelph, Guelph, Ontario N1G 2W1, Canada

Received August 23, 2005; Revised Manuscript Received November 20, 2005

ABSTRACT: Modification of the bacterial cell wall heteropolymer peptidoglycan by addition of an acetyl group to the C-6 hydroxyl group of *N*-acetylmuramoyl residues is known to inhibit the activity of muramidases (lysozymes) of innate immune systems. The O-acetylation of peptidoglycan also precludes the action of intrinsic lytic transglycosylases, enzymes that require a free C-6 hydroxyl group to generate their 1,6-anhydromuropeptide products. This class of autolysins is ubiquitous in peptidoglycan-synthesizing bacteria as they are responsible for insertion of pores and flagella, spore formation, and the general metabolism of peptidoglycan. We recently discovered a cluster of genes in the *Neisseria gonorrhoeae* chromosome that are proposed to participate in peptidoglycan O-acetylation (Weadge, J. T., Pfeffer, J. M., and Clarke, A. J. (2005) *BMC Microb. 5*, 49). In the current study, we demonstrate that one of these genes, *ape1* functions as an *O*-acetylpeptidoglycan esterase. The *ape1* gene was cloned and overexpressed in *Escherichia coli* as a fusion protein with a hexa-histidine tag. The expressed protein was purified to apparent homogeneity and assayed for activity as an esterase using three different assays involving high-performance liquid chromatography and chromogenic detection methods which measured the release of ester-linked acetate from a variety of polymer and soluble substrates. These assays demonstrated that Ape1 has a higher specific activity on O-acetylated peptidoglycan compared to O-acetylated xylan. Consequently, Ape1 represents the first enzyme characterized as an *O*-acetylpeptidoglycan esterase. The physicochemical and kinetic parameters of Ape1 were determined using soluble chromogenic substrates for convenience. Thus, its pH optima for stability and activity were observed to be 6.0 and 6.2, respectively, while its optimum temperature for activity was 55 °C. Two forms of truncated Ape1 are generated in *E. coli*, one lacked the complete predicted N-terminal signal sequence, while the second involved a proteolytic cleavage within this signal sequence. The smaller truncated form was localized predominantly to the periplasm, whereas the larger form was mainly associated with the outer membrane, and to a lesser extent, the cytoplasmic membrane, sites expected for the maintenance of peptidoglycan.

The structural rigidity and shape of bacteria is conferred by a sacculus of peptidoglycan which completely surrounds the cytoplasmic membrane. This unique cell wall heteropolymer is comprised of alternating *N*-acetylglucosaminyl-β-1,4-*N*-acetylmuramoyl residues with attached peptide. The presence of the latter permits interpeptide cross-linking between neighboring strands of peptidoglycan to provide a continuous three-dimensional macromolecule that withstands the internal turgor pressure of the cell. Given its essential role in the vitality of bacterial cells, the peptidoglycan sacculus is the target of lytic enzymes such as lysozyme (muramidases), which are released by a eukaryotic host as the first line of defense against invasion. As seen elsewhere in nature, such as with the xylans of plant cell walls (reviewed in ref *1*), the decoration of peptidoglycan with simple aglycon moieties provides protection from lytic action. For many pathogenic bacteria, this modification involves the O-acetylation of the C-6 hydroxyl group of muramoyl residues (reviewed in refs *2*, *3*) (Figure 1).

The O-acetylation of peptidoglycan occurs in many bacteria, both Gram-positive and Gram-negative, including a number of important human pathogens such as *Staphylococcus aureus*, *Neisseria gonorrhoeae*, and *N. meningitidis* (*2*, *3*). The findings of a recent study have added species of *Campylobacter*, *Helicobacter*, and *Bacillus*, including *B. anthracis*, to this list (*4*). The extent of this modification varies with species and strain, but typically falls within the range of 20−70% (relative to muramoyl residues) (*2*−*4*). O-Acetylated peptidoglycan has been shown to evade degradation by lysozymes in a concentration-dependent manner (*5*−*9*). On the basis of structural information obtained by X-ray crystallography with lysozyme−substrate complexes and theoretical considerations, it is thought that the presence of the acetyl groups at the C-6 hydroxyl of muramoyl residues would preclude productive binding of peptidoglycan in subsites B, D, and/or F of lysozyme's active site (*5*). The consequences of this inhibition can be significant as the persistence of O-acetylated peptidoglycan within the mammalian host has been shown to lead to complement activation, pyrogenicity, somnogenesis, and arthrogenicity (*2*, *3*).

In addition to blocking the action of host muramidases of the innate immune system, O-acetylation also influences the

† This research was supported by an operating grant (MOP 62772) to A.J.C. from the Canadian Institutes of Health Research and a post-graduate scholarship (PGSB) to J.T.W. from the Natural Sciences and Engineering Research Council of Canada.

* To whom correspondence should be addressed: E-mail, aclarke@uoguelph.ca; phone, 519-824-4120; fax, 519-837-1802.

10.1021/bi051679s CCC: $33.50
Published on Web 12/24/2005

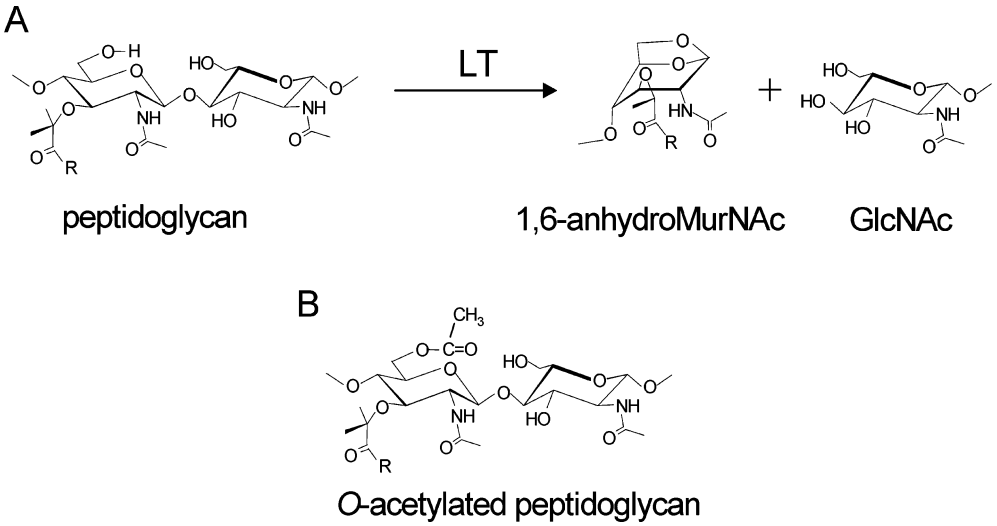

FIGURE 1: Reaction catalyzed by lytic transglycosylases and structure of O-acetylated peptidoglycan. (A) The lytic transglycosylases (LT) cleave peptidoglycan between the *N*-acetylmuramoyl (MurNAc) and *N*-acetylglucosaminyl (GlcNAc) residues of peptidoglycan to produce 1,6-anhydroMurNAc and GlcNAc. The R denotes the stem peptide on MurNAc residues. (B) The O-acetylation of peptidoglycan occurs at the C-6 hydroxyl group of MurNAc residues, thereby precluding the formation of 1-6-anhydroMurNAc by LT activity.

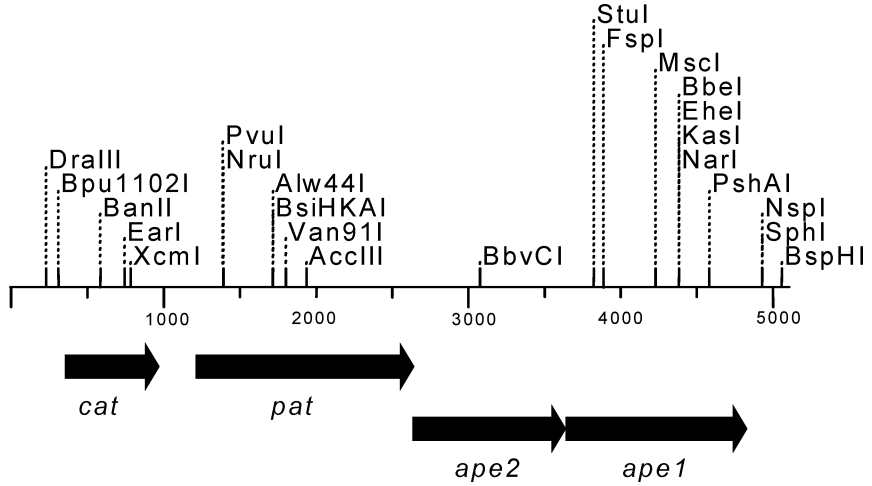

FIGURE 2: Genetic organization and restriction enzyme map of OAP cluster. Ape, *O*-acetylpeptidoglycan esterase; pat, peptidoglycan *O*-acetyltransferase; cat, chloramphenicol acetyltransferase (*4*).

activity of bacterial autolysins (*10*), enzymes involved in the biosynthesis and turnover of peptidoglycan, insertion of appendages, and secretion systems (recently reviewed in refs *11*, *12*). This is especially the case for the major class of autolysin involved with these processes, the lytic transglycosylases. Whereas these enzymes act on peptidoglycan at the same site as lysozyme (viz. specifically between MurNAc and GlcNAc residues), the lytic transglycosylases are not hydrolases but instead cleave the β-1,4 linkage with the concomitant formation of 1,6-anhydormuramoyl residues (Figure 1) (*13*). Thus, the presence of free C-6 hydroxyl groups on muramoyl residues is a strict requirement for lytic transglycosylase activity.

Given that the lytic transglycosylases, together with the penicillin-binding proteins, have been demonstrated to comprise complexes involved in peptidoglycan biosynthesis (*12*, *14*), it would be expected that bacteria possess a means to specifically remove O-linked acetate as required, but there is a dearth of information about the pathway for the O-acetylation of peptidoglycan, and nothing is known regarding its removal. Early studies with both *Proteus mirabilis* and *N. gonorrhoeae* indicated O-acetylation to be a maturation event that closely follows after the incorporation of new strands into the peptidoglycan sacculus (*15*). This implies that a source of acetate from within the cytoplasm would have to be transported across the cytoplasmic membrane prior to being attached to the newly ligated muramoyl residues in peptidoglycan.

We recently reported the discovery of a gene cluster within the genomes of a number of bacteria that O-acetylate their peptidoglycans, including *N. gonorrhoeae*, which encode hypothetical proteins that may participate in this process (Figure 2) (*4*). Sequence alignment searches suggested that at least one of the open reading frames within the respective clusters encodes a hypothetical protein with similarity to *O*-acetylxylan esterases. As *N. gonorrhoeae* does not utilize xylan or cellulose as a carbon source, nor does it possess a xylanolytic system of enzymes, we proposed that this protein functions as an *O*-acetylpeptidoglycan esterase (Ape)[1] which

[1] Abbreviations: APE, *O*-acetylpeptidoglycan esterase; *p*NP, *p*-nitrophenyl; MeUm, 4-methylumbelliferyl; αNA, α-naphthyl, pat, peptidoglycan *O*-acetyltransferase; cat, chloramphenicol acetyltransferase.

Table 1: Bacterial Strains and Plasmids Used in This Study

strain or plasmid	relevant characteristics[a]	reference or source
E. coli strains		
DH5α	K-12 ϕ80d *lacZ*ΔM15 *endA1 hsdR17* (r_K^- m_K^-) *supE44 thi-1 gyrA96 relA1* p(*lacZYA-argF*) U169 F^-	Life Technologies, Inc.
BL21[λDE3] pLysS	F^- *ompT hsdS*$_B$ (r_B^- m_B^-) *gla dcm met* (DE3) pLysS (Cm^R)	Novagen
ACJW14	BL21[λDE3] pLysS harboring pJWAC14	this study
ACJW16	BL21[λDE3] pLysS harboring pJWAC16	this study
P. stuartti PR50		*51*
N. gonnorheae FA1090		*52*
FA 62		*53*
CH811		*54*
plasmids		
pET30a(+)	IPTG inducible expression vector; Km^R	Novagen
pET28A(+)	IPTG inducible expression vector	Novagen
pACJW13	pET28a(+) derivative containing *ape1* on a *NcoI/HindIII* fragment; Km^R	this study
pACJW14	pET28 a(+) derivative containing corrected *ape1* on a *NcoI/HindIII* fragment; Km^R	this study
pACJW16	pET28 a(+) truncated derivative of *ape1* lacking N-terminal signal sequence of 20 amino acid residues on a *NcoI/HindIII* fragment; Km^R	this study
pACJW17	pJWAC14derivative containing Km^R cassette from pET30a; Km^R	this study

[a] Cm^R and Km^R, resistance to chloramphenicol and kanamycin, respectively.

acts on peptidoglycan to remove *O*-acetyl groups. This study presents data in support of this hypothesis and thus represents the first report of an *O*-acetylpeptidoglycan esterase.

EXPERIMENTAL PROCEDURES

Chemicals and Reagents. DNase I, RNase A, Pronase, IPTG, and EDTA-free protease inhibitor tablets were purchased from Roche Molecular Biochemicals (Laval, PQ, Canada), while Fisher Scientific (Nepean, ON, Canada) provided acrylamide, glycerol, pyridine, and Luria Bertani (LB) growth medium. All other growth media were purchased from Difco Laboratories (Detriot, MI). Mono S 5/5 and Superdex 75 were purchased from Amersham Pharmacia Biotech (Uppsala, Sweden), and Ni^{2+}NTA-agarose was a product of Qiagen (Valencia, CA). T_4 DNA ligase and restriction enzymes were from New England Biolabs (Mississauga, ON, Canada), and unless otherwise stated, all other chemicals and reagents were from Sigma Chemical Co. (St. Louis, MO).

O-Acetylated peptidoglycan was isolated from *Providencia stuartii* PR50 (used because of its relatively high *O*-acetyl content), treated with α-amylase, DNase I, RNase A, and heat-treated Pronase, and then purified as previously described (*16*). Commercially available birchwood xylan (Fluka) was per-acetylated with acetic anhydride in pyridine for 48 h at room temperature. Solubilization of the per-acetylated xylan was then accomplished by heating in 25 mM sodium phosphate buffer, pH 6, at 70 °C for 1 h according to the method of Johnson et al. (*17*). Following exhaustive dialysis against 16 L of 25 mM sodium phosphate buffer, pH 6, the O-acetylated xylan preparation was lyophilized and stored until required.

Bacterial Strains and Growth Media. The sources of plasmids and bacterial strains used in this study, together with their genotypic description, are listed in Table 1. *N. gonorrhoeae* strains FA1090, FA62, and CH811 were used for PCR amplification of genes, sequence specific mutagenesis, and/or complementation experiments. They were all grown for 24 h at 35 °C in an anaerobic container on GC medium base supplemented with Kellogg's defined supplement (*18*, *19*) in a humid, 5% CO_2 environment. This medium was supplemented with kanamycin (18 μg/mL) and chloramphenicol (5 μg/mL) where appropriate. *Escherichia coli* DH5α and *P. stuartii* PR50 were maintained on LB broth or agar at 37 °C. *E. coli* BL21-λDE3 (pLysS), used for protein expression, was maintained on LB agar containing 35 μg/mL chloramphenicol. For the expression of high levels of proteins, *E. coli* BL21-λDE3 was grown in Super Broth (5 g of sodium chloride, 20 g of yeast extract, and 32 g of tryptone) at 37 °C with agitation. All strains were maintained for long periods by storage at −70 °C in 25% glycerol.

Identification and Genomic Analysis of an O-Acetyl Peptidoglycan (poa) Gene Cluster. The raw nucleotide sequence data of the *N. gonorrhoeae* FA1090 genome project (*20*) was searched for hypothetical proteins involved in acetate transport using the *Pseudomonas aeruginosa* protein sequence for AlgI as the probe (*algI* encodes a putative acetate translocator involved with the biosynthesis of alginate (*21*)). Identification of open reading frames, protein translations, and isoelectric points (p*I*) were performed using Clone Manager 5. Signal sequence predictions were performed using signalP version 2 (http://www.cbs.dtu.dk/services/SignalP-2.0/). Searches for homologues to the characterized *N. gonorrhoeae* genes were carried out using the NCBI protein−protein BLAST database to tentatively identify functions for each of the genes in the cluster (http://www.ncbi.nlm.nih.gov/BLAST/). Protein alignments were performed using ClustalW Version 1.8 software (http://www.ebi.ac.uk/clustalw), and shading was done using BOXSHADE Version 3.21 (http://www.ch.embnet.org/software/BOX_form.html).

Cloning of ape1. Whole cells from an overnight GCMBK plate culture of *N. gonorrhoeae* FA1090 were diluted with double-distilled H_2O to adjust optical density at 550 nm of the suspension to 0.5. This suspension was used as the chromosomal DNA template for PCR amplification. Oligonucleotide primers (prepared by the Guelph Molecular Supercenter) were designed for the PCR amplification of *ape1* and Δ*ape1*, a truncated derivative lacking the predicted N-terminal signal sequence, from the *N. gonorrhoeae* strains FA1090, FA62, and CH811. Restriction sites for cloning were incorporated into both the forward and complementary reverse primers. For *ape1*, the forward primer (5′-ATCTAGTACACACAG CCATGGACCCCAAACACTTC-3′) intro-

duced an *Nco*I site (underlined) that mutated the codon following the start codon for the gene; however, this change was needed for cloning of the gene into pET28a(+). The complementary reverse primer (5′-CCCCTGACAAGCTTTGCCTGATTGCG-3′) introduced a *Hind*III site (underlined) that mutated the stop codon. For Δ*ape1*, the forward primer (5′-CCACGCACGCCATGGCACTGCCCCG-3′) introduced an *Nco*I site (underlined) following the signal sequence, and the complementary reverse primer was the same as above. PCR amplifications were performed with the Expand Long Template Polymerase kit from Roche Molecular Biochemicals according to the manufacturer's specifications. The resulting *ape1* and Δ*ape1* PCR products were digested with *Nco*I and *Hind*III and ligated into the matching restriction sites of pET28a(+), generating plasmids pACJW13 and pACJW16, respectively. Site-directed mutagenesis was performed to correct the codon following the start codon in the *ape1* gene sequence so that it matched the chromosomal sequence coding for an asparagine. Thus, the coding (5′-GGAGATATA CCATGAACCCCAAACACTTC-3′) and noncoding primers (5′-GAAGTGTTTGGGGTTCAT GGTATATCTCC-3′) were prepared and used according to the manufacturers specifications for the QuikChange site-directed mutagenesis kit (Stratagene), thereby generating plasmid pACJW14. DNA sequence analysis ensured that the cloned segment had the correct sequence. The pACJW14 plasmid construct was engineered such that its expression produced a C-terminal hexa-histidine tagged Ape1 protein. Expression of Δ*ape1* from pACJW16 produced an Ape1 derivative (Δape1) which also possessed a C-terminal hexa-histidine tag but lacked an N-terminal signal sequence.

Production and Purification of Ape1 and Δ*ape1*. For the overexpression of both *ape1* and Δ*ape1*, *E. coli* BL21 (DE3 pLysS) cells transformed with pACJW14 or pACJW16 (generating *E. coli* ACJW14 and ACJW16, respectively) were grown in SuperBroth at 37 °C to an OD_{600} of 0.6 and then induced for 3 h at 18 °C with the addition of IPTG to a final concentration of 1 mM. Cells were isolated by centrifugation (5000*g*, 15 min, 4 °C) and stored at −20 °C until needed. To purify the His_6-tagged proteins, cell pellets were thawed and resuspended in a minimal volume of lysis buffer (50 mM sodium phosphate, pH 8, and 500 mM sodium chloride). Lysozyme (1 mg/mL), RNase A (10 μg/mL), and DNase I (5 μg/mL) were added to aid lysis, and EDTA-free protease inhibitor tablets (1 per 15 mL of suspension) were added to prevent protein degradation. The suspension was incubated at 4 °C for 30 min before being subjected to sonication (intervals of 5 s bursts with 10 s cooling periods for a total of 2 min). Unlysed cells were removed from the lysate by centrifugation (5000*g*, 15 min, 4 °C), and 1 mL of Ni^{2+}NTA-agarose was added for every 10 mL of cleared lysate. The mixtures were incubated for 1 h at 4 °C with shaking before being applied to 15-mL disposable plastic columns. Unbound proteins in the mixtures were allowed to flow through, and the matrix was subsequently washed with approximately 10 column vol of lysis buffer. The matrix was further washed with approximately 10 column vol of wash buffer 1 (50 mM sodium phosphate, pH 8, 500 mM sodium chloride, and 20 mM immidazole) and 10 column vol of wash buffer 2 (50 mM sodium phosphate, pH 8, 500 mM sodium chloride, and 30 mM immidazole). Bound proteins were then batch-eluted from the column in 10 mL of elution buffer (50 mM sodium phosphate, pH 8, 500 mM sodium chloride, and 75 mM immidazole). The eluted protein mixtures were dialyzed for 16 h against 2 × 4 L of 25 mM sodium phosphate buffer, pH 7.

The His_6-tagged Ape1 and Δape1 were further purified by cation-exchange chromatography on MonoS. Protein was applied to the column following its equilibration in running buffer (25 mM sodium phosphate buffer, pH 7.0) at a flow rate of 1 mL/min. Elution of protein from the column was accomplished by increasing the ionic strength of the running buffer using a linear 0−1 M NaCl gradient. The His_6-tagged proteins eluted in buffer containing approximately 75 mM NaCl.

Zymogram Analysis. Zymogram analysis was performed essentially as described by Rosenberg et al. (*22*) and Degrassi et al. (*23*) using 2 mM α-naphthyl acetate (αNA-acetate) in 25 mM phosphate buffer, pH 7.0, as substrate. After incubation for 15 min, gels were stained with 0.5% tetrazotized *O*-dianisidine in the same phosphate buffer.

Enzyme Assays. For routine detection of acetyl esterase activity, 2 mM *p*-nitrophenol acetate (*p*NP-acetate) in 50 mM sodium phosphate buffer, pH 7.0, was used as substrate in a 96-well microtiter plate assay. Reactions involving a total volume of 300 μL were initiated by the addition of the *p*NP-acetate and were allowed to proceed for at least 5 min. The reaction progress was monitored at 405 nm for the appearance of *p*-nitrophenol.

The specificity of His_6-tagged Ape1 on both soluble and insoluble polymeric substrates was investigated by incubating the enzyme with the substrates in 50 mM sodium phosphate buffer, pH 7.0, at 37 °C. With O-acetylated peptidoglycan substrates, the insoluble material was sonicated for 1 min continuously to generate an evenly dispersed solution. Final reaction mixtures contained 5 mg/mL O-acetylated peptidoglycan in the phosphate buffer containing 0.1% Triton X-100. All assays were stopped by acidifying reaction mixtures with 1 M H_2SO_4, and then insoluble material was removed by centrifugation (5000*g*, 10 min) prior to analysis for liberated acetate. Samples of peptidoglycan incubated in the absence of added enzyme served as controls for the spontaneous release of acetate.

Three methods were employed for the quantification of released acetic acid: HPLC-based organic acid analysis (*24*) using an Aminex HPX-87H Bio-Rad column, a coupled enzymatic assay using a commercially available kit according to the manufacturer's specifications (Boehringer Mannheim), and the colorimetric assay for esters developed by Hestrin (*25*). One unit (U) of activity is defined as the amount of enzyme required to produce 1 μmol of product in 1 min, and specific activities are reported as the average of at least three independent trials.

The Michaelis−Menten parameters of both Ape1 and Δape1 were determined for *p*NP-acetate and αNA-acetate using concentrations ranging from 0.05 to 8 mM. Plots of initial reaction velocities as a function of substrate concentration were analyzed by nonlinear regression using the Microcal Origin 6.0 program and assuming a one-site binding model.

Dependence of Ape1 Stability and Activity on Temperature and pH. To determine the effect of temperature on His_6-tagged Ape1 stability, samples of enzyme in 50 mM phosphate buffer, pH 7.0, were incubated at temperatures

ranging from 25 to 65 °C for 24 h. At 15 min intervals, aliquots were removed and assayed at 37 °C for activity using *p*NP-acetate as substrate. The optimal temperature for activity was determined by assaying the enzyme in the same buffer at increasing temperatures to 65 °C.

For the determination of the effects of pH on stability, the His_6-tagged Ape1 enzyme was incubated for 1 h in buffers ranging from pH 3 to 8.0 (100 mM sodium acetate, pH 3.0 to 5.5; 100 mM sodium phosphate, pH 5.0 to 8.0). Reaction volumes were then adjusted to pH 7.0, and the activity was assayed using *p*NP-acetate at pH 7.0 as substrate. The optimal pH for activity was determined by assaying the enzyme in the pH range from 3 to 8 (25 mM sodium acetate, pH 3.0 to 5.5; 25 mM sodium phosphate, pH 5.0 to 8.0).

Localization Studies of Ape1. The cellular localization of His_6-tagged Ape1 was investigated by Western immunoblotting using an anti-His_6 antibody (Santa Cruz Biotechnologies) and alkaline phosphatase detection after the SDS−PAGE separation of isolated cell fractions. Membrane fractions were purified as described previously (*26*, *27*) with some modifications. Following the overexpression of His_6-tagged Ape1 from a 1 L culture of *E. coli* ACJW14, the cells were harvested by centrifugation (5000*g*, 15 min, 4 °C). The cell pellet was resuspended in 20 mL of 100 mM HEPES, pH 7.8, containing lysozyme (1 mg/mL), RNase A (10 μg/mL), DNase I (5 μg/mL), 2 EDTA-free protease inhibitor tablets, and 20% sucrose and incubated at 4 °C for 30 min before being passed through a French Pressure cell twice at 18 000 psi. Unruptured cells were removed from the suspension by centrifugation (5000*g*, 15 min, 4 °C). The supernatant was applied to a sucrose step gradient (1 mL of 72% sucrose and 3 mL of 15% sucrose in 30 mM Tris buffer, pH 8.0) and subjected to ultracentrifugation at 183 000g for 1 h in a Beckman SW 41 rotor. Membranes were removed from the interface with a syringe, and 1.5 mL was layered onto a second sucrose step gradient (0.9 mL of 72% sucrose, 1.1 mL of 65% sucrose, 3 mL of 50% sucrose, 3 mL of 35% sucrose, and 1.5 mL of 25% sucrose in 30 mM Tris buffer, pH 8.0). The second gradient was again subjected to ultracentrifugation at 183 000g for 18 h, and the separated membrane bands were removed with syringes. Each membrane fraction was subsequently washed four times with sterile deionized H_2O and collected by ultracentrifugation (183 000*g*, 1 h) between washings. The membrane pellets were then resuspended in a minimum volume of sterile deionized H_2O and stored at −20 °C until required.

Periplasmic and cytoplasmic fractions were purified from separate batches of cells grown and induced as above. The pelleted cells were resuspended in 20 mL of 30 mM Tris buffer, pH 8.1, containing 20% sucrose and treated with lysozyme (1 mg/mL) and 10 mM EDTA (final concentration). Following incubation at 4 °C for at least 30 min, the periplasmic components were recovered in the supernatant after centrifugation (5000*g*, 15 min, 4 °C) and stored at −20 °C. The cell pellet was frozen and then thawed to aid in lysis before being resuspended in 30 mL of 3 mM EDTA, pH 7.3, containing RNase A (10 μg/mL), DNase I (5 μg/mL), and 2 EDTA-free protease inhibitor tablets. The suspension was sonicated for intervals of 5 s bursts with 10 s cooling periods for a total of 2 min. Unlysed cells were removed from the lysate by a low-speed centrifugation (5000*g*, 15 min, 4 °C), and then membranes were removed by ultracentrifugation (160 000*g*, 1 h). The supernatant containing cytoplasmic components was stored at −20 °C.

As indicators of purity of the various cell fractions, each fraction was tested in triplicate for the presence of NADH oxidase (cytoplasmic membrane) and 2-keto-3-deoxyoctonate (KDO) (outer membrane) using the methods of Osborn et al. (*28*) and Karkhanis et al. (*29*), respectively.

Chromosomal Mutation of ape1 in N. gonorrhoeae. Creation of an insertional mutant of *ape1* in *N. gonorrhoeae* was based on a protocol established in the Dillon laboratory (*30*, *31*) and involved two separate PCR events. First, the *ape1* gene on pACJW14 was modified to incorporate unique restriction sites using inverse PCR. Briefly, this involved the amplification of the entire plasmid outward from the middle of the *ape1* gene. The coding primer (5′-GCGCCTGCAG-**GCCGTCTGAA**CGAAATGGCGTGCCGAC-3′) contained a *Pst*I site (underlined) and an *N. gonorrhoeae* uptake sequence (boldface). The noncoding primer (5′-GCGCGG-TACC**GCCGTCTGAA**GTTGACGGTCAGGGTTTGTTCG-3′) contained a *Kpn*I site (underlined) and an *N. gonorrhoeae* uptake sequence (boldface). The second PCR event was the amplification of the kanamycin resistance cassette from pET30a using the forward primer (5′-GCGCGGTAC-CTTTCTCATAGCTCACGCTG-3′) and the complementary reverse primer (5′-GCGCCTGCAGTTCAAATATGTATC-CGCTC-3′) containing *Kpn*I and *Pst*I sites (underlined), respectively. The *Kpn*I−*Pst*I digeted amplicons from both PCRs were ligated together to form pACJW17, which would act as a suicide vector in *N. gonorrhoeae*. DNA sequence analysis ensured that both the insertion and orientation of the kanamycin resistance cassette were correct. Three strains of *N. gonorrhoeae*, (CH811, FA1090, and FA62) were transformed with pACJW17 according to the protocol described by Janik et al. (*32*). Transformants were selected on GCMBK media supplemented with kanamycin and screened for successful gene replacement by PCR analysis.

Other Analytical Techniques. Protein concentrations were determined using a bicinchoninic acid assay (Pierce, Rockford, IL). SDS−PAGE was performed by the method of Laemmli (*33*) using 12% acrylamide gels and Coomassie Brilliant Blue staining. Matrix-assisted laser-desorption ionization time-of-flight (MALDI-TOF) mass spectrometry was performed on the purified protein samples at the Biological Mass Spectrometry Facility, University of Guelph, following their exchange into 10 mM ammonium acetate buffer, pH 7.0, using YM30 microcon filtration units. Amino-terminal protein sequencing was performed at both the Institute of Biological Sciences, National Research Council of Canada, Ottawa, and the NAPS Unit, University of British Columbia, Canada.

RESULTS

Initial Identification of ape1 and Its Deduced Amino Acid Sequence. *N. gonorrhoeae* is known to O-acetylate its peptidoglycan (*9*); however, the genes involved in this process remain unknown. To help identify potential genes associated with *O*-acetylation, a BLAST search of the *N. gonorrhoeae* genome was conducted using *algI*, a *P. aeruginosa* gene encoding a putative acetate transporter involved with the O-acetylation of its extracellular alginate (*21*, *34*) as the probe. A homologue of AlgI with 33% amino acid

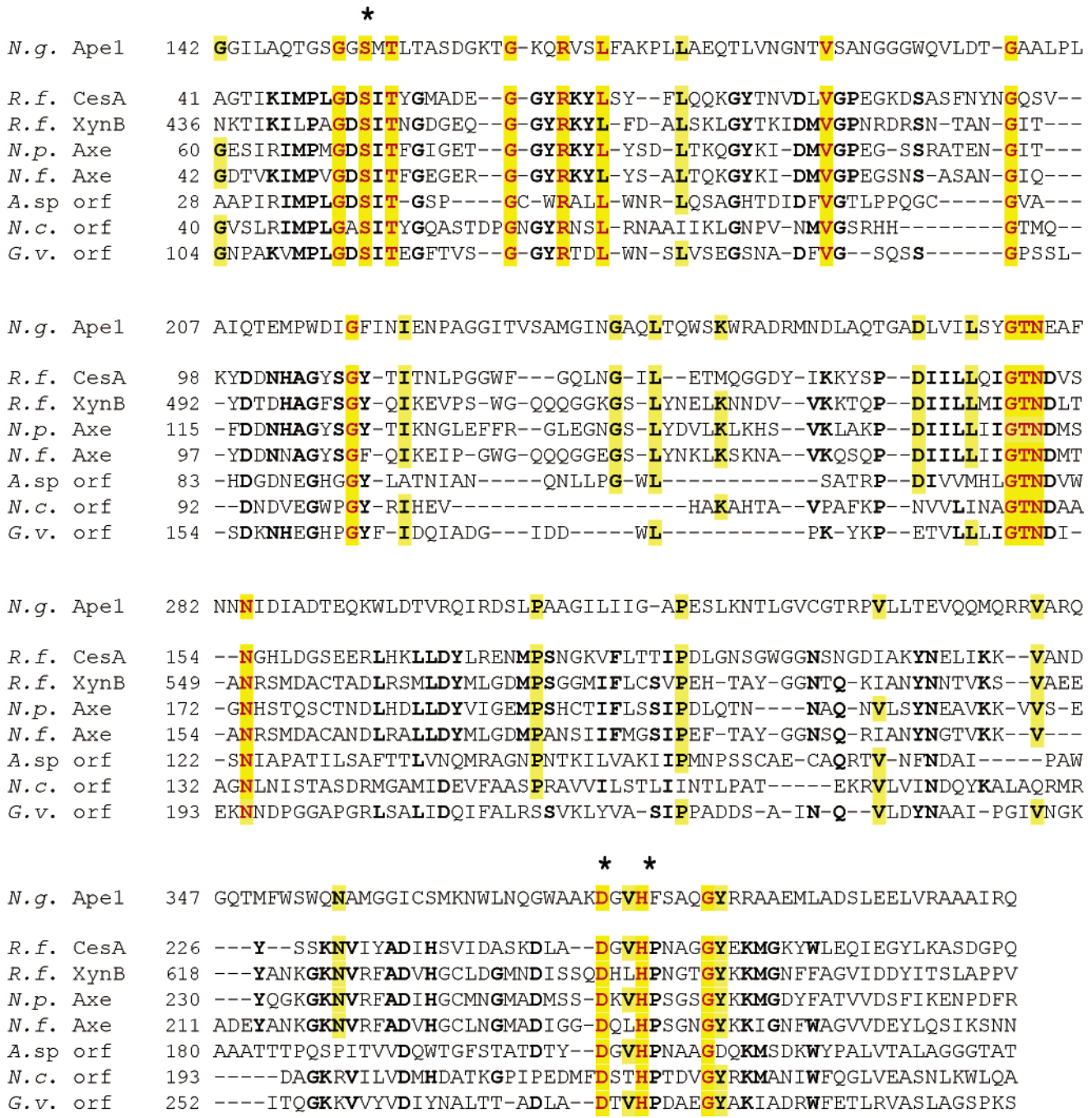

FIGURE 3: Amino acid sequence alignment of the CE3 carbohydrate esterases and Ape1. Residues common to at least 50% of acetylxylan esterases are in boldface, those with identity to Ape1 are hatched, and invariant residues among all sequences are in red. The asterisks denote the possible identities of the residues comprising the catalytic triad of the active sites of the respective enzymes. Abbreviations (accession numbers): *N.g.*, *N. gonorrhoeae* FA1090 (AAW89270); *R.f.*, *Rumminococcus flavefaciens* (CesA, Q9RLB8; XynB, Q52753); *N.p.*, *Neocallimastix patriciarum* (O13497); *N.f.*, *Neocallimastix frontalis* (AAQ10006.1); *A.*sp., *Actinomadura* sp. (Q7WZ50); *N.c.*, *Neurospora crassa* (XP_323879.1); *G.v.*, *Gloeobacter violaceus* (Q7NGX3).

identity (51% similarity) was discovered in the raw sequence data of the unfinished genome project of *N. gonorrhoeae* FA1090 (*20*). This ORF was found to be associated with a potential cluster of ORFs with hypothetical functions associated with *O*-acetyl groups on carbohydrates (Figure 2). The 3′-end of one of these ORFs (accession number AAW89270) involving 1193 nucleotides encoded a hypothetical protein with 48% similarity to an acetyl xylan esterase (EC 3.1.1.72) from *Ruminococcus flavefaciens*, an enzyme which belongs to the family 3 carbohydrate esterases (CE3) of the CAZy classification (http://afmb.cnrs-mrs.fr/CAZY) (*35*). Alignment of the *N. gonorrhoeae* ORF sequence with each of the CE3 esterases led to the identification of conserved sequence motifs (Figure 3). We note that this ORF does not share sequence similarities to peptidoglycan *N*-acetylglucosamine deacetylases (EC 3.1.1.-) from *Streptococcus pneumoniae* (*36*) and *Bacillus cereus* (*37*), members of family CE4, or the recently discovered *N*-acetylmuramic acid deacetylase (EC 3.5.1.-) from *Bacillus subtilis* (*38*).

Each of the other members of family CE3 are acetyl xylan esterases (EC 3.1.1.72); no de-*N*-acetylases belong to this

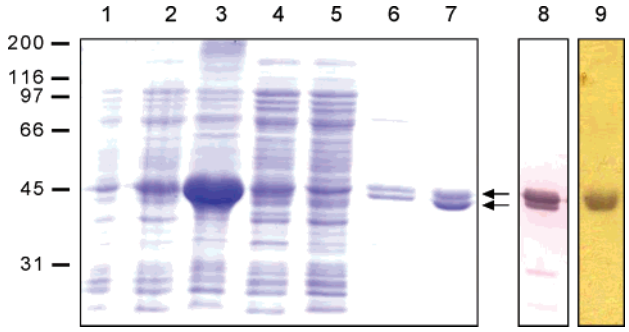

FIGURE 4: Purification of Ape1 and zymogram analysis of esterase activity. Lanes 1−7, SDS−PAGE analysis (staining with Coomassie Brilliant Blue) of fractions isolated at different stages of purification. Lane 1, uninduced cell-culture lysate (soluble and insoluble material); lane 2, cell-culture lysate following 3-h induction with 1 mM IPTG; lane 3, unlysed cells and insoluble material following lysis by sonication; lane *4*, cell lysate following ultracentrifugation; lane 5, flow-through fraction from immobilized metal-ion affinity column; lane 6, eluted fraction from the immobilized metal-ion affinity column; and lane 7, eluted protein from chromatography on Mono S. The two arrows denote the mobility of the two forms of isolated Ape1, and the molecular markers (kDa) are indicated on the left. Lane 8, Western immunoblot of lane 7 using anti-His6 antibody to detect the purified His_6-tagged Ape1. Lane 9, zymogram analysis of purified Ape1 fraction using αNA-acetate as the substrate to detect esterase activity.

family. As *N. gonorrhoeae* is not a xylanolytic bacterium and its genome does not appear to encode xylanases, we postulated that the hypothetical esterase functions on peptidoglycan to specifically catalyze de-O-acetylation. We tentatively named this gene *ape1* for *O*-acetylpeptidoglycan esterase 1 (EC 3.1.1.x). *Ape1* encodes a hypothetical protein of 44 087 Da and with a p*I* of 8.72. Analysis of the predicted amino acid sequence using the SignalP program indicates the presence of an N-terminal signal sequence of 20 amino acid residues. A second ORF immediately upstream from *ape1* was found to share 17.3% identity and 39.7% similarity with Ape1 at the amino acid sequence level. This ORF was tentatively named Ape2 (*20*), but its activity and function are currently unknown.

Cloning and Expression of ape1. The entire *ape1* gene was amplified by PCR using *N. gonorrhoeae* genomic DNA as template, and it was subsequently cloned into the *E. coli* protein overexpression system, pET28(+). However, nucleotide sequencing of the resulting construct, pACJW13, revealed sequence anomalies when compared to the unfinished genome sequence. Multiple PCR amplifications and sequencing of *ape1* from three *N. gonorrhoeae* strains, FA1090, CH811, and FA62, were performed to confirm the correct gene sequence. Once established, the correct gene was then cloned into pET28a(+) to generate plasmid pACJW14.

Optimal production of His_6-tagged Ape1 from *E. coli* BL21[MDE3] pLysS freshly transformed with pACJW14 generating *E. coli* ACJW14 was obtained after induction with 1 mM IPTG followed by a 3-h incubation at 18 °C. This lower induction temperature was required to maintain the solubility of a larger fraction of the expressed protein. When SDS−PAGE analysis was used, significant amounts of protein expression were evident by the intense band located at approximately 42 kDa in Coomassie Blue-stained gels (hypothetical, 44 kDa) (Figure 4). The expressed enzyme

Table 2: Purification of Ape1 and Δape1[a]

enzyme fraction	total protein (mg)	total activity[b] (μmol·min^{-1})	specific activity[b] (μmol·min^{-1}·mg^{-1})	purification (fold)	yield (%)
		Ape1			
cell lysate	278	106	0.381	1	100
Ni^{2+}-NTA agarose	2.34	13.4	5.72	15	12.6
Mono S	0.36	3.59	9.98	26.3	3.39
		Δape1			
cell lysate	532	81.1	0.152	1	100
Ni^{2+}-NTA agarose	10.7	23.2	2.16	14.2	28.6
Mono S	2.12	21.7	10.2	67.1	26.8

[a] Enzyme purification from 1 L cultures of *E. coli* ACJW14 (Ape1) and ACJW16 (Δape1). [b] Activity assayed using 2 mM *p*NP-acetate as substrate in 50 mM sodium phosphate buffer, pH 7.0, at 25 °C.

was released from cells disrupted by sonication, but large amounts remained in the insoluble fraction as aggregates. However, enough of the His_6-tagged Ape1 was still present in the soluble fraction to proceed with its purification. Confirmation for the presence of the His tag was obtained by Western immunoblotting using a monoclonal antibody specific for the tag (Figure 4, lane 8).

Purification of Ape1. Immobilized metal affinity chromatography on Ni^{2+}NTA-agarose was employed as the first step for the purification of Ape1. As seen in Figure 4, this resulted in the isolation of the majority of the enzyme present in the soluble, crude fraction, but both higher and lower molecular weight contaminants were present. As Ape1 is predicted to have a relatively high p*I* value of 8.72, cation-exchange chromatography was selected for the second purification step. Chromatography of the partially purified Ape1 on MonoS successfully removed the contaminating proteins and thus provided apparent homogeneous preparations of the enzyme (Figure 4).

As seen in Figure 4, Ape1 was purified in two distinguishable forms. Both were demonstrated to be active as acetyl esterases by zymogram analysis, and both were shown to possess the His_6 tag as detected by Western immunoblotting (Figure 4). Given the C-terminal location of the hexa-His tag, these data suggest that the two isolated proteins are distinct derivatives of the same enzyme that presumably has been N-terminally processed. The combined purified preparation of these two forms of enzyme was found to have a specific activity of 9.98 μmol/(min·mg protein) using *p*NP-acetate as a substrate which represents a 26-fold purification factor (Table 2). The overall yield of 3.4% is quite low and reflects the fact that much of the total produced protein was lost as insoluble precipitates.

NH_2-Terminal Sequencing and Mass Spectrometry. In silico analysis of the Ape1 sequence using the program Signal P indicated the presence of a signal sequence involving the 20 N-terminal residues with a cleavage site between Ala20 and Leu21 (Figure 5). Thus, in an attempt to confirm that the two isolated proteins represented individual derivatives of the same enzyme, the combined enzyme fraction was subjected to NH_2-terminal sequencing. Unfortunately, however, no sequence could be obtained for either protein even after multiple attempts by two independent sequencing facilities, indicating that the proteins may be N-terminally modified in some fashion. Whether this modification occurs

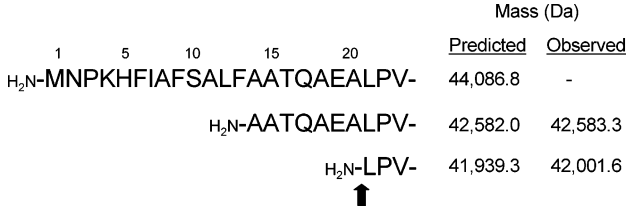

FIGURE 5: N-Terminal sequence and mass of Ape1 and its isolated derivatives. The arrow denotes the predicted cleavage site.

naturally or arises during the handling and purification of the enzyme is currently not known.

Analysis of the enzyme preparation by MALDI-TOF mass spectrometry provided molecular masses of 42 583 and 42 002 Da. The full-length Ape1 including its predicted signal sequence has a theoretical mass of 44 089 Da, thus, indicating that both isolated forms of the enzyme had been processed. The lower mass corresponded to that expected for truncated Ape1 lacking its predicted signal sequence (Met1−Ala20). The second and higher mass corresponded (within 1 mass unit) to a truncated derivative of the enzyme which includes the seven C-terminal amino acid residues of the signal sequence, indicating the presence of a second cleavage site between residues Phe13 and Ala14.

*Production and Purification of Truncated Ape1 (*Δ*ape1*). Given the variable processing of wild-type *N. gonorrhoeae* Ape1 in transformed *E. coli*, a truncated derivative of the enzyme lacking the entire N-terminal signal sequence of 20 amino acid residues was engineered. Thus, cells of *E. coli* BL21[*λ*DE3] pLysS freshly transformed with pACJW16 harboring Δ*ape1* were grown to late exponential phase and harvested. The expressed protein was isolated and purified as for Ape1 with a respectable overall yield of 26.8% (Table 2) and was analyzed kinetically as described below.

Specificity of Ape1. The specificity of Ape1 was investigated by incubating the enzyme with various acetylated substrates and monitoring the release of acetate by three different assays. When the synthetic substrate *p*NP-Ac was used, the specific activity of Ape1 was determined to be 9.98 *μ*mol/min which was, within experimental error, identical to that for ΔApe1 (Table 2). For this reason, subsequent studies involved only Ape1.

In addition to being active on *p*NP-Ac, Ape1 also catalyzed the hydrolysis of αNA-acetate with almost the same specific activity (Table 3). Interestingly, the enzyme was considerably more active on 4-methylumbelliferyl-acetate (MeUm-acetate), indicating its preference for more complex substrates in terms of the acetyl carrier moiety. In contrast, activity was barely detectable with either butyrate or decanoate serving as the carrier, indicating that Ape1 is not a lipase.

In terms of potential natural substrates, Ape1 was tested as an acetylxylan esterase using peracetylated birch wood xylan at pH 7.0 as substrate. As shown in Figure 6, the enzyme was observed to release acetate from a 5 mg/mL suspension of the substrate, and an average specific activity of 1.4 nmol/(min·mg protein) was calculated. However, the enzyme was more active on O-acetylated peptidoglycan isolated from *P. stuartii* at the same concentration (Figure 6). Moreover, Ape1 released more acetate from this latter substrate, even though the effective concentration of acetate is lower given its presence is only associated with the C-6 of muramoyl residues of the heteropolymeric peptidoglycan compared to the C-2 and C-3 of every xylose residue of the peracetylated xylan homopolymer. These data are significant because, previously, authentic acetylxylan esterases have been shown to be totally devoid of activity on peptidoglycan (*39*, *40*). No release of acetate was detected when the enzyme was incubated for extended periods of time with either chemically de-O-acetylated *P. stuartii* peptidoglycan (prepared by prior treatment with 10 mM NaOH) or *E. coli* peptidoglycan which is not O-acetylated naturally (*5*). In addition, Ape1 did not release acetate from chitin, chitooligosaccharides (degree of polymerization, 2−6), or *N*-acetylglucosamine (Table 3, Figure 6). Taken together, these data confirm that Ape1 does not act as either a lipase or an *N*-acetylglucosamine deacetylase but instead functions as an *O*-acetyl esterase. Thus, this is the first report of an *O*-acetylpeptidoglycan esterase.

Table 3: Enzymatic Specificity of Ape1

substrate	specific activity[a] (μmol·min^{-1}·mg^{-1})
*p*NP-acetate	9.98 ± 0.21
*p*NP-butyrate	$4.49 \times 10^{-4} \pm 7.8 \times 10^{-5}$
*p*NP-decanoate	$6.93 \times 10^{-4} \pm 9.8 \times 10^{-5}$
αNA-acetate	6.29 ± 0.26
MeUm-acetate	247 ± 76
peracetylated xylan	1.36 ± 0.34
O-AcPG	1.63 ± 0.61
PG	ND[b]
MurNAc	ND[b]
GlcNAc	ND[b]
$(GlcNAc)_6$	ND[b]
chitin	ND[b]

[a] Enzyme in 50 mM sodium phosphate buffer, pH 7.0, was incubated at 37 °C with soluble substrates at 2 mM concentration or 5 mg/mL for insoluble substrates. [b] ND, not detected.

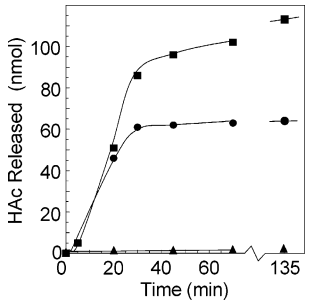

FIGURE 6: Time course of Ape1-catalyzed release of acetate release from insoluble substrates. The enzyme in 50 mM phosphate buffer, pH 7.0, at 37 °C was incubated with 5 mg/mL of (●) peracetylated birch wood xylan, (■) *O*-acetylated *P. stuartii* PG, or (▲) either de-O-acetylated PG, *E. coli* PG, or chitin. At the times indicated, aliquots were removed and released acetic acid from the insoluble substrates was quantified using the HPLC assay. Representative data are presented.

Characterization of Enzymatic Properties. For convenience, the dependence of Ape1 activity and stability on pH and temperature was determined using the synthetic substrate *p*NP-acetate. As seen in Figure 7, Ape1 activity was found to have a temperature optimum of 55 °C, but the enzyme was only stable for any extended period of time (up to 24 h) at temperatures below 37 °C. Thus, incubation of the enzyme for just 1 h at 50 °C resulted in greater than 60% loss of original activity. The enzyme could be maintained at −20 °C for extended periods of time (more than 4 weeks) without the loss of activity.

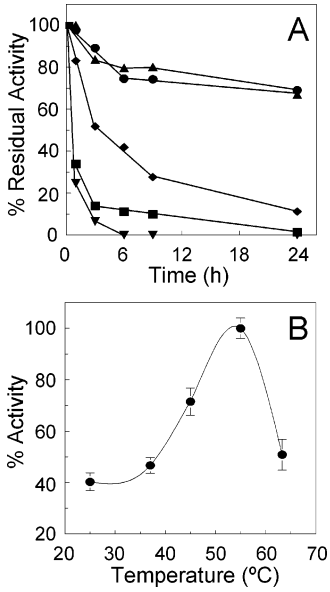

FIGURE 7: Effect of temperature on Ape1 stability and activity. (A) The stability of Ape1 was determined by incubating enzyme samples in 50 mM phosphate buffer, pH 7.0, at 25 (●), 37 (▲), 45 (◆), 50 (■), and 55 °C (▼) for 24 h. At the times indicated, aliquots were removed and assayed at 37 °C for activity using *p*NP-acetate as substrate. The data are presented as averages of three trials. (B) The optimal temperature for activity was determined by assaying the enzyme in the same buffer for 5 min at the temperatures indicated. The error bars denote SD ($n = 6$).

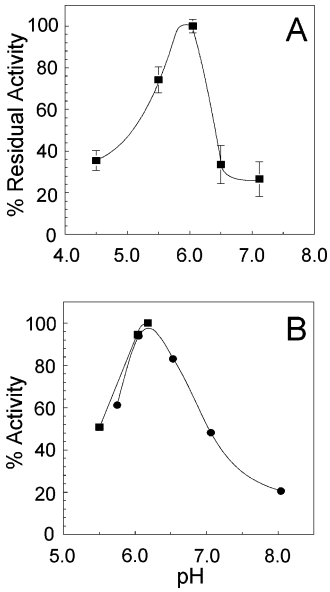

FIGURE 8: Effect of pH on Ape1 stability and activity. (A) The stability of Ape1 was determined by incubating enzyme samples for 1 h in buffers ranging from pH 4.5 to 7.1 at 25 °C and then assaying for activity using *p*NP-acetate in 50 mM phosphate buffer, pH 7.0, as substrate. (B) The optimal pH for activity was determined by assaying the enzyme at 25 °C in (■) 25 mM sodium acetate and (●) 25 mM sodium phosphate buffers at the indicated pH values. The error bars denote SD ($n = 6$).

Ape1 was stable over a relatively narrow range of pH centered at 6.0 (Figure 8). After incubation for 1 h at pH 5.5 and 6.5, less than 70% and 40% residual activity, respectively, was observed. For the determination of the dependence of the enzyme's activity on pH, correction had to be made for the affect of pH on the absorption coefficient of the chromogenic *p*-nitrophenol. Thus, individual absorption coefficients for *p*-nitrophenol were determined at the various pHs tested and applied to calculate each respective reaction rate. A plot of these reaction rates as a function of pH was bell-shaped with the optimal pH for Ape1 activity centered at 6.2. However, we note that this experiment was complicated by the facts that *p*NP-acetate undergoes spontaneous hydrolysis at pH values above 7 and the rate of this hydrolysis increases with increasing pH. Thus, while the background of the spontaneous hydrolysis was accounted for in the calculations, it is likely that its increasing rate begins to significantly compromise the analysis of the enzyme-catalyzed reaction. For this reason, the pH study was limited to conditions of pH 8 and below.

Table 4: Kinetic Parameters of Ape1[a]

	substrate	K_M (mM)	V/E_t (s^{-1})	V/E_tK_M ($mol^{-1}\cdot s^{-1}$)
Ape1	αNA-acetate	0.27 ± 0.08	3.99 ± 0.28	1.48×10^4
	*p*NP-acetate	0.53 ± 0.12	6.95 ± 0.34	1.31×10^4
Δape1	*p*NP-acetate	0.66 ± 0.09	7.85 ± 0.26	1.12×10^4

[a] Reactions were conducted in 50 mM sodium phosphate buffer, pH 7.0, at 25 °C.

Table 5: Cellular Localization of Ape1 in *E. coli* Acjw14[a]

cellular fraction	KDO (μmol)	specific activity: NADH oxidase ($nmol\cdot min^{-1}\cdot mg^{-1}$)	specific activity: Ape1[b] ($\mu mol\cdot min^{-1}\cdot mg^{-1}$)
cytoplasm	1.14 ± 0.67	0.0086 ± 0.00052	0.121 ± 0.0046
inner membrane	1.35 ± 0.035	22.4 ± 0.32	0.0284 ± 0.0015
periplasm	1.30 ± 0.43	8.70 ± 0.12	0.142 ± 0.0011
outer membrane	22.4 ± 0.21	2.66 ± 0.024	0.0482 ± 0.0029

[a] Contents associated with cells from a 1 L culture. [b] Detected as total esterase activity using 2 mM *p*NP-acetate as substrate in 50 mM sodium phosphate buffer, pH 7.0, at 25 °C.

Given the intrinsic problems associated with using insoluble peptidoglycan as a substrate for detailed kinetic analyses (*16*), the Michaelis−Menten parameters of Ape1 were determined for only the two chromogenic synthetic substrates *p*NP-acetate and αNA-acetate. As expected from specific activity measurements, the overall efficiency of the enzyme acting on the two substrates was virtually the same, as reflected by V/E_tK_m values (Table 4). Likewise, very little difference in both the V/E_t and K_m values was noted between Ape1 and Δape1 when acting on *p*NP-acetate as substrate.

Cellular Localization of Ape1. To investigate the cellular localization of Ape1, various cell fractions of *E. coli* ACJW14 were prepared by density gradient ultracentrifugation and then analyzed by SDS−PAGE and Western immunoblotting, taking advantage of the C-terminal His_6 tag for its identification. Following the two density gradient centrifugation steps, we obtained three distinct membrane bands. NADH oxidase and KDO assays confirmed that, as expected, the low-density band corresponded to the inner membrane (extent of contamination less than 10% (*28*)), the high-density band was the outer membrane, and the middle-density band comprised a mixture of both (Table 5). The two pure membrane fractions were isolated and, together with the isolated periplasmic and cytoplasmic fractions, were analyzed for the presence of Ape1 (Figure 9, Table 5). These analyses revealed that the smaller truncated form of the enzyme was predominantly localized to the periplasm, whereas the larger truncated form was mainly associated with

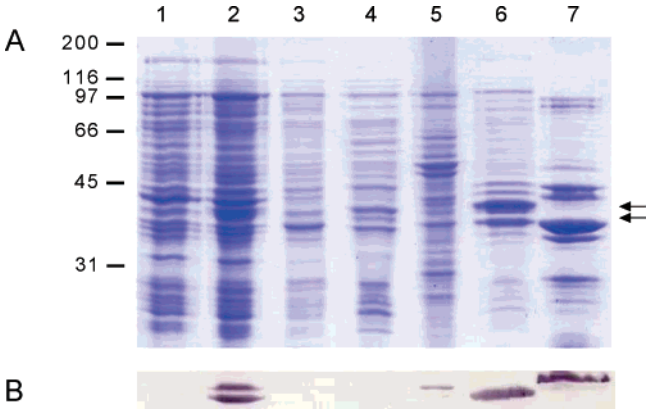

FIGURE 9: Cellular localization of Ape1 in *E. coli*. (A) Coommassie Brilliant Blue stained SDS−PAGE gel loaded with different cellular fractions of *E. coli*. Lane 1, uninduced cell-culture lysate; lane 2, cell-culture lysate following 3-h induction with 1 mM IPTG; lane 3, cell culture supernatant; lane 4, cytoplasmic fraction; lane 5, low-density cytoplasmic membrane fraction; lane 6, periplasmic fraction; and lane 7, high-density, outer membrane fraction. The two arrows denote the mobility of the two forms of isolated Ape1. Molecular markers (kDa) are indicated on the left. (B) Corresponding Western immunoblot using anti-His_6 antibody to detect His_6-tagged Ape1 in the cell fractions.

the outer membrane, and to a lesser extent, the cytoplasmic membrane. These data are consistent with the requirement of the enzyme's activity on peptidoglycan to permit the unimpeded action of the lytic transglycosylases which are directly associated with the inner leaflet of the outer membrane and form complexes with the penicillin-binding proteins associated with the outer leaflet of the cytoplasmic membrane (*12*). In control experiments, esterase activity was not detected in cellular fractions obtained from *E. coli* BL21 harboring pET28A(+).

Inactivation of ape1 in N. gonorrhoeae. To investigate the importance and physiological function of the Ape1 in *N. gonorrhoeae*, attempts were made to mutate its chromosomal gene by insertion of a kanamycin cassette using the allelic exchange strategy described by Pagotto et al. (*19*). To facilitate the directional insertion of the kanamycin cassette amplified from pET30a(+) into *ape1*, the gene sequence on pACJW14 was modified to include the necessary unique restriction sites. By this process, 78 base pairs were removed from the middle of *ape1* by the insertion of the cassette, but more than 400 bases pairs remained on either side of the cassette to allow for homologous recombination. This plasmid, named pACJW17, served as the suicide vector for the transformation of three *N. gonorrhoeae* strains, FA1090, FA62, and CH811. Selection for transformants on GCMBK supplemented with kanamycin yielded very few colonies, and PCR analysis revealed that none of these experienced a successful double crossover event. These transformations were repeated several times with no success suggesting that *ape1* may be essential for the viability of *N. gonorrhoeae*.

DISCUSSION

Whereas *N*-acetylglucosamine deacetylases associated with peptidoglycan metabolism have been described in the literature since their discovery in 1957 (*41*), this is the first report of an *O*-acetyl esterase with specificity directed toward peptidoglycan. Moreover, our inability to disrupt the chromosomal *ape1* gene provides strong, albeit indirect, evidence that the enzyme is important for the viability of *N. gonorrhoeae*, a bacterium that O-acetylates its peptidoglycan. This view is consistent with the important role that the lytic transglycosylases play in the biosynthesis, maintenance, and modification of peptidoglycan as Ape1 would serve to remove *O*-acetyl groups on muramoyl residues thereby controlling and/or permitting the unimpeded action of the lytic enzymes. Indeed, the lytic transglycosylases strictly require a free hydroxyl group on C-6 of muramoyl residues for their activity leading to the formation of 1,6-anhydromuramoyl product. The localization of Ape1 to the periplasm and its possible association with both the cytoplasmic and outer membranes is consistent with this important and, presumably, essential functional role.

Ape1 was initially identified as an acetyl xylan esterase based on sequence comparisons (*4*), and it can be assigned to family CE3 of the carbohydrate esterases which, to date, is composed of enzymes with specificity only to acetyl xylan. This assignment is primarily based on sequence similarities to conserved motifs associated with putative active site residues of these esterases, including catalytic residues, which would be largely conserved regardless of the substrate specificity of the respective enzymes. The xylan substrate of these enzymes is a plant cell wall polymer of β-1,4-D-xylose that, similar to the more decorated β-1,4-linked peptidoglycan polymer, can be substituted to various degrees with *O*-acetyl groups which serve to protect the polymer from the hydrolytic action of xylanases. The xylans are themselves produced to form layers over the main structural plant cell-wall polymer cellulose thereby protecting it from cellulolytic enzymes (*1*). The esterases are thus required and produced by xylanolytic microorganisms for the efficient hydrolysis of both xylan and cellulose (*40*). Given that *N. gonorrhoeae* is neither xylanolytic or cellulolytic, the physiological function of Ape1 must be different, and this was borne out in our investigation of its substrate profile. A comparison of its specific activity with those of authentic acetyl xylan esterases indicated that Ape1 is relatively inefficient when acting on xylan. However, in contrast to the other esterases, Ape1 is more active on peptidoglycan than xylan; in fact, authentic acetyl xylan esterases are devoid of activity on this complex heteropolymer (*39*, *40*). This situation is analogous to the ability of lysozyme to hydrolyze peptidoglycan as its natural substrate and, to a lesser extent, the more structurally simple homopolymer chitin (poly *N*-acetylglucosamine), while chitinases are only able to act on the latter. Thus, Ape1 is proposed to de-esterify peptidoglycan as its true substrate but can accommodate the more simple acetylated xylan in its active site, while the converse is not possible for authentic acetylxylan esterases.

Despite their discovery almost 20 years ago (*42*), not much is really known about the mechanism of action of the acetyl xylan esterases. Sequence alignment studies have indicated the existence of a number of invariant amino acid residues within the various families of the enzymes, but no structure−function studies have been performed. However, the three-dimensional structures of the catalytic core of the family 5 acetylxylan esterases from *Hypocrea jecorina* (formerly *Trichoderma reesei*) (PDB 1QOZ) (*43*) and *Penicillium purporogenum* (PDB 2AXE) (*44*) have been determined. Modeling studies based on the *H. jecorina* esterase structure

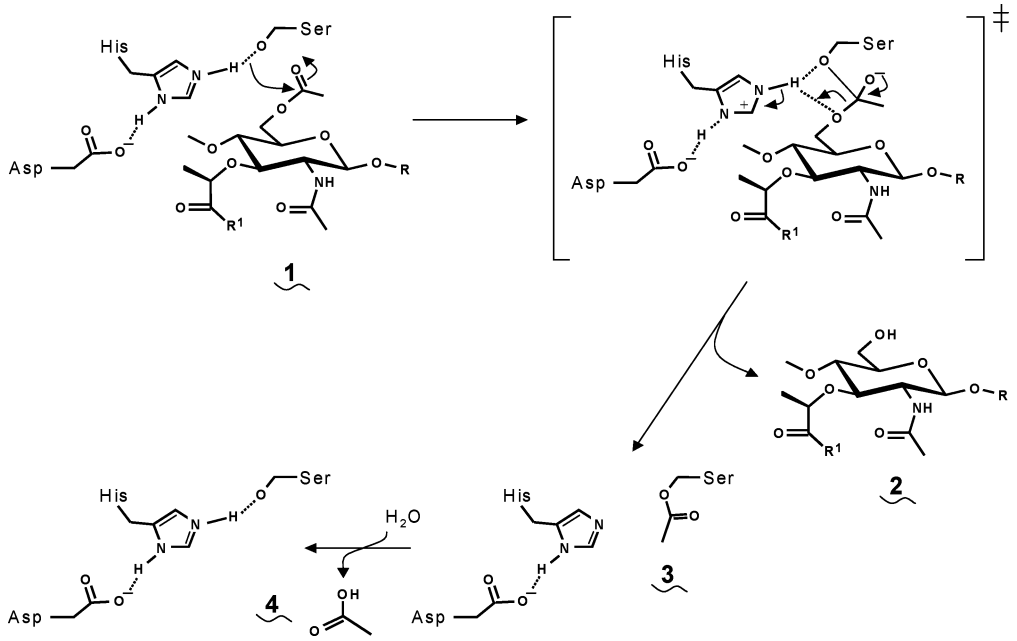

FIGURE 10: Catalytic mechanism proposed for the hydrolysis of ester-linked acetate from *O*-acetylmuramyl residues by Ape1. A catalytic His residue which is salt-bridged to an Asp removes a proton from the hydroxyl group of a catalytic Ser rendering its oxygen nucleophilic. The nucleophilic oxygen is poised to attack the carbonyl carbon of the acetyl group of the esterified muramoyl residue of the peptidoglycan substrate (**1**) to form a tetrahedral intermediate which subsequently collapses to form an acyl enzyme intermediate (**3**) with the concomitant release of the free muramoyl product (**2**). The acyl enzyme is then hydrolyzed through a reversal of the process to liberate the acetate product (**4**) and return the catalytic Ser residue to its protonated state.

together with both structural and biochemical data obtained with another family 5 esterase, a cutinase from *Fusarium solani* (EC 3.1.1.x; PDB 1CUS) (*45*), have provided some insight into a possible mechanism which is proposed to follow that of classical serine proteases/esterases involving a catalytic triad of conserved amino acids (*43*). Thus, a basic His residue which is salt-bridged to an Asp removes a proton from the hydroxyl group of a Ser rendering its oxygen nucleophilic (Figure 10). This nucleophilic oxygen then attacks the carbonyl carbon of the acetyl group of an ester substrate (**1**) to form a tetrahedral intermediate which collapses to form an acyl enzyme intermediate (**3**) with the concomitant release of the free sugar product (**2**). The acyl enzyme is then hydrolyzed through a reversal of the process to liberate the acetate product (**4**) and return the Ser residue to its protonated state. Alignment of the family 3 enzymes does indicate the presence of invariant Asp, His, and Ser residues (Figure 3), and so it is tempting to speculate that Ape1 and the other family 3 carbohydrate esterases also function as classical serine esterases involving the participation of this triad in a charge relay system.

The pH optimum of 6.2 for the activity of Ape1 acting on the chromogenic substrates is similar to that observed for other *O*-acetyl esterases including the *P. purpurogenum* acetylxylan esterase (*46*). This pH optimum and the bell shape of the curve for Ape1 activity as a function of pH are consistent with the proposed mechanism of action of the enzyme involving ionizable residues. However, while candidate catalytic residues exist within the conserved motifs of the family 3 carbohydrate esterases, further detailed investigation is required to confirm their participation in a catalytic triad involving the charge relay mechanism.

Mass spectrometric analysis of purified Ape1 revealed that it was expressed in recombinant *E. coli* as two N-terminally truncated forms. The higher molecular mass form was found to be associated with both the cytoplasmic and outer membranes and would appear to have been generated by cleavage at an unpredicted processing site. This processing of Ape1 and its resulting retention of a membrane anchor may be simply an artifact of the high protein expression levels associated with the recombinant *E. coli* as differential signal sequence processing of another *O*-acetyl esterase expressed in *E. coli* has been demonstrated previously by Blum and co-workers (*47*). Similarly, Poutanen and Sundberg also found that the *H. jecorina* acetylxylan esterase was expressed as two isoforms (*48*). With Ape1, cellular processing at its predicted cleavage site led to the production of a soluble enzyme that remained in the periplasm and available to deacetylate peptidoglycan in the sacculus. The enzyme may remain free to serve this function or perhaps associate with the multienzyme complex(es) comprised of the lytic transglycosylases and penicillin-binding proteins that function to catalyze the final stages of peptidoglycan biosynthesis (*49*−*52*). By formation of this association, the activity of the esterase would be confined only to regions on the peptidoglycan sacculus that are being remodeled and/or synthesized and thus would provide an elegant means for the cell to control its action. This possible association of Ape1 with multienzyme complexes is currently under investigation.

Attempts to inactivate the chromosomal copy of *ape1* in *N. gonorrhoeae* were unsuccessful. The protocol adopted to generate the insertional mutant has been used previously to investigate cell division in *N. gonorrhoeae* (*30*, *31*). In these earlier studies, the chromosomal genes encoding the cell-division proteins MinC and MinD were disrupted successfully to help delineate their function in the division process. With *ape1*, it is conceivable that the insertion of the kanamycin cassette into the gene affected the polarity of one or more downstream genes. Alternatively, and more likely,

Ape1 may be essential for cell viability. This would be consistent with the presumed role of the enzyme in providing sites for the unimpeded activity of the lytic transglycosylases and other autolysins.

We have previously shown that various bacterial autolysins are inhibited by the presence of O-linked acetate on peptidoglycan (*10*). These enzymes are essential for the biosynthesis of the sacculus during cell growth, and its localized remodeling for the insertion of flagella, pili, and transport systems (*11*) and failure to remove this acetate by Ape1 may result in bacteriostasis or even cell death. For this reason, we believe that Ape1 may serve as a new potential target for the development of a new class of antibiotics specific for important human pathogenic bacteria.

ACKNOWLEDGMENT

We thank David Watson, National Research Council of Canada, for help and advice with N-terminal amino acid sequencing and Dyanne Brewer for her skillful technical assistance with MALDI-TOF MS. We also thank Jo-Ann Dillon and Sandra Ramirez-Arcos, University of Ottawa, for advice and assistance with the generation of the insertional mutant of *ape1*.

REFERENCES

1. Clarke, A. J. (1996) *Biodegradation of Cellulose: Enzymology and Biotechnology*. CRC Press, Boca Raton, FL.
2. Clarke, A. J., Strating, H., and Blackburn, N. T. (2000) Pathways for the *O*-acetylation of bacterial cell wall polysaccharides, in *Glycomicrobiology* (Doyle, R. J., Ed.) pp 187−223, Plenum Publishing Co. Ltd., New York.
3. Clarke, A. J., and Dupont, C. (1992) *O*-Acetylated peptidoglycan: its occurrence, pathobiological significance and biosynthesis, *Can. J. Microbiol. 38*, 85−91.
4. Weadge, J. T., Pfeffer, J. M., and Clarke, A. J. (2005) Identification of a new family of enzymes with potential *O*-acetylpeptidoglycan esterase activity in both Gram-positive and Gram-negative bacteria, *BMC Microbiol. 5*, 49.
5. Dupont, C., and Clarke, A. J. (1991) Dependence of lysozyme-catalysed solubilization of *Proteus mirabilis* peptidoglycan on the extent of *O*-acetylation, *Eur. J. Biochem. 195*, 763−769.
6. Swim, S. G., Gfell, M. A., Wilde, C. E., III, and Rosenthal, R. S. (1983) Strain distribution in extents of lysozyme resistance and *O*-acetylation of gonococcal peptidoglycan determined by high-performance liquid chromatography, *Infect. Immun. 42*, 446−452.
7. Rosenthal, R. S., Folkening, W. J., Miller, D. R., and Swim, S. C. (1983) Resistance of *O*-acetylated gonococcal peptidoglycan to human peptidoglycan-degrading enzymes, *Infect. Immun. 40*, 826−829.
8. Rosenthal, R. S., Blundell, J. K., and Perkins, H. R. (1982) Strain-related differences in lysozyme sensitivity and extent of O-acetylation of gonococcal peptidoglycan, *Infect. Immun. 37*, 826−829.
9. Blundell, J. K., Smith, G. J., and Perkins, H. R. (1980) The peptidoglycan of *Neisseria gonorrhoeae*: *O*-acetyl groups and lysozyme sensitivity, *FEMS Microbiol. Lett. 9*, 259−261.
10. Payie, K. G., Strating, H., and Clarke, A. J. (1996) The role of *O*-acetylation in metabolism of peptidoglycan in *Providencia stuartii*, *Microb. Drug Resist.* 2, 135−140.
11. Koraimann, G. (2003) Lytic transglycosylases in macromolecular transport systems of Gram-negative bacteria, *Cell. Mol. Life Sci. 60*, 2371−2388.
12. Höltje, J.-V. (1998) Growth of the stress-bearing and shape-maintaining murein sacculus of *Escherichia coli*, *Microbiol. Mol. Biol. Rev. 62*, 181−203.
13. Höltje, J.-V., Mirelmen, D., Sharon, N., and Schwarz, U. (1975) Novel type of murein transglycosylase in *Escherichia coli*, *J. Bacteriol. 124*, 1067−1076.
14. von Rechenberg, M., Ursinus, A., and Höltje, J.-V. (1996) Affinity chromatography as a means to study multi-enzyme complexes involved in murein synthesis. *Microb. Drug Resist. 2*, 155−157.
15. Snowden, M. A., Perkins, H. R., Wyke, A. W., Hayes, M. V., and Ward, J. B. (1989) Cross-linking and *O*-acetylation of newly synthesized peptidoglycan in *Staphylococcus aureus* H, *J. Gen. Microbiol. 135*, 3015−3022.
16. Blackburn, N. T., and Clarke, A. J. (2002) Characterization of soluble and membrane-bound family 3 lytic transglycosylases from *Pseudomonas aeruginosa*, *Biochemistry 41*, 1001−1013.
17. Johnson, K. G., Fontana, J. D., and MacKenzie, C. R. (1988) Measurement of acetylxylan esterase in Streptomyces, *Methods Enzymol. 160*, 551−560.
18. Kellogg, D. S., Jr., Peacock, J. R., Deacon, W. F., Brown, L., and Pirkle, C. I. (1963) *Neisseria gonorrhoeae*. I. Virulence genetically linked to clonal variation, *J. Bacteriol. 85*, 1274−1279.
19. Pagotto, F., Salimnia, H., Totten, P. A., and Dillon, J. R. (2000) Stable shuttle vectors for *Neisseria gonorrhoeae*, *Haemophilus* spp. and other bacteria based on a single origin of replication, *Gene 244*, 13−19.
20. Roe, B. A., Lin, S. P., Song, L., Yuan, X., Clifton, S., Ducey, T., Lewis, L., and Dyer, D. W. (2001) Gonococcal genome sequencing project.
21. Nivens, D. E., Ohman, D. E., Williams, J., and Franklin, M. J. (2001) Role of alginate and its *O* acetylation in formation of *Pseudomonas aeruginosa* microcolonies and biofilms, *J. Bacteriol. 183*, 1047−1057.
22. Rosenberg, M., Roegner, V., and Becker, F. F. (1975) The quantitation of rat serum esterases by densitometry of acrylamide gels stained for enzyme activity, *Anal. Biochem. 66*, 206−212.
23. Degrassi, G., Kojic, M., Ljubijankic, G., and Venturi, V. (2000) The acetyl xylan esterase of *Bacillus pumilus* belongs to a family of esterases with broad substrate specificity, *Microbiology 146*, 1585−1591.
24. Clarke, A. J. (1993) Extent of peptidoglycan *O*-acetylation in the tribe *Proteeae*, *J. Bacteriol. 175*, 4550−4553.
25. Hestrin, S. (1949) The reaction of acetylcholine and other carboxylic acid derivatives with hydroxylamine, and its analytical application *J. Biol. Chem. 180*, 249−261.
26. Hancock, R. E. W., and Nikaido, H. (1978) Outer membranes of gram-negative bacteria. XIX. Isolation from *Pseudomonas aeruginosa* PAO1 and use in reconstitution and definition of the permeability barrier, *J. Bacteriol. 136*, 381−390.
27. Horstman, A. L., and Kuehn, M. J. (2000) Enterotoxigenic *Escherichia coli* secretes active heat-labile enterotoxin via outer membrane vesicles, *J. Biol. Chem. 275*, 12489−12496.
28. Osborn, M. J., Gander, J. E., Parisi, E., and Carson, J. (1972) Mechanism of assembly of the outer membrane of *Salmonella typhimurium*. Isolation and characterization of cytoplasmic and outer membrane, *J. Biol. Chem. 247*, 3962−3972.
29. Karkhanis, Y. D., Zeltner, J. Y., Jackson, J. J., and Carlo, D. J. (1978) A new and improved microassay to determine 2-keto-3-deoxyoctonate in lipopolysaccharide of Gram-negative bacteria, *Anal. Biochem. 85*, 595−601.
30. Ramirez-Arcos, S., Szeto, J., Beveridge, T. J., Victor, C., Francis, F., and Dillon, J. (2001) Deletion of the cell-division inhibitor MinC results in lysis of *Neisseria gonorrhoeae*, *Microbiology 147*, 225−237.
31. Szeto, J., Ramirez-Arcos, S., Raymond, C., Hicks, L. D., Kay, C. M., and Dillon, J. A. (2001) Gonococcal MinD affects cell division in *Neisseria gonorrhoeae* and *Escherichia coli* and exhibits a novel self-interaction. *J. Bacteriol. 183*, 6253−6264.
32. Janik, A., Juni, E., and Heym, G. A. (1976) Genetic transformation as a tool for detection of *Neisseria gonorrhoeae*, *J. Clin. Microbiol. 4*, 71−81.
33. Laemmli, U. K. (1970) Cleavage of structural proteins during the assembly of the head of bacteriophage T4, *Nature 227*, 680−685.
34. Franklin, M. J., and Ohman, D. E. (1996) Identification of *algI* and *algJ* in the *Pseudomonas aeruginosa* alginate biosynthetic gene cluster which are required for alginate *O*-acetylation, *J. Bacteriol. 178*, 2186−2195.
35. Coutinho, P. M., and Henrissat, B. (1999) Carbohydrate-active enzymes: an integrated database approach, in *Recent Advances in Carbohydrate Bioengineering* (Gilbert ,H. J., Davies, G., Henrissat, B., and Svensson, B., Eds.), pp 3−12, The Royal Society of Chemistry, Cambridge, U.K.
36. Vollmer, W., and Tomasz, A. (2000) The *pgdA* gene encodes for a peptidoglycan *N*-acetylglucosamine deacetylase in *Streptococcus pneumoniae*, *J. Biol. Chem. 275*, 20496−20501.
37. Psylinakis, E., Boneca, I. G., Mavromatis, K., Deli, A., Hayhurst, E., Foster, S. J., Varum, K. M., and Bouriotis, V. (2005)

Peptidoglycan *N*-acetylglucosamine deactetylases from *Bacillus cereus*, highly conserved proteins in *Bacillus anthracis*, *J. Biol. Chem.*, *280*, 30856−30863.
38. Fukushima, T., Kitajima, T., and Sekiguchi, J. (2005) A polysaccharide deacetylase homologue, PdaA, in *Bacillus subtilis* acts as an *N*-acetylmuramic acid deacetylase *in vitro*, *J. Bacteriol. 187*, 1287−1292.
39. Caufrier, F., Martinou, A., Dupont, C., and Bouriotis, V. (2003) Carbohydrate esterase family 4 enzymes: substrate specificity, *Carbohydr. Res. 338*, 687−692.
40. Dupont, C., Daigneault, N., Shareck, F., Morosoli, R., and Kluepfel, D. (1996) Purification and characterization of an acetyl xylan esterase produced by *Streptomyces lividans*, *Biochem. J. 319*, 881−886.
41. Roseman, S. (1957) Glucosamine metabolism. I. *N*-acetylglucosamine deacetylase, *J. Biol. Chem. 226*, 115−124.
42. Biely, P., Puls, J., and Schneider, H. 1985. Acetyl xylan esterases in fungal cellulolytic systems, *FEBS Lett. 186*, 80−84.
43. Hakulinen, N., Tenkanen, M., and Rouvinen, J. (2000) Three-dimensional structure of the catalytic core of acetylxylan esterase from *Trichoderma reesei*: insights into the deacetylation mechanism, *J. Struct. Biol. 132*, 180−190.
44. Ghosh, D., Sawicki, M., Lala, P., Erman, M., Pangborn, W., Eyzaguirre, J., Gutierrez, R., Jornvall, H., and Thiel, D. J. (2001) Multiple conformations of catalytic serine and histidine in acetylxylan esterase at 0.90 Å, *J. Biol Chem. 276*, 11159−11166.
45. Longhi, S., Czjzek, M., amzin, V., Nicolas, A., and Cambillau, C. (1997) Atomic resolution (1.0 Å) crystal structure of *Fusarium solani* cutinase: stereochemical analysis, *J. Mol. Biol. 268*, 779−799.
46. Egana, L., Gutierrez, R., Caputo, V., Peirano, A., Steiner, J., and Eyzaguirre, J. (1996) Purification and characterization of two acetyl xylan esterases from *Penicillium purpurogenum*, *Biotechnol. Appl. Biochem. 1996*, 33−39.
47. Blum, D. L., Li, X. L., Chen, H., and Ljungdahl, L. G. (1999) Characterization of an acetyl xylan esterase from the anaerobic fungus *Orpinomyces* sp. strain PC-2, *Appl. Environ. Microbiol. 65*, 3990−3995.
48. Poutanen, K., and Sundberg, M. (1988) An acetyl esterase of *Trichoderma reesei* and its role in the hydrolysis of acetyl xylans, *Appl. Microbiol. Biotechnol. 28*, 419−424.
49. Höltje, J.-V. (1996) Molecular interplay of murein synthases and murein hydrolases in *Escherichia coli*, *Microb. Drug Resist. 2*, 99−103.
50. Höltje, J.-V. (1996) A hypothetical holoenzyme involved in the replication of the murein sacculus of *Escherichia coli*, *Microbiology 142*, 1911−1918.
51. von Rechenberg, M., Ursinus, A., and Höltje, J.-V. (1996) Affinity chromatography as a means to study multienzyme complexes involved in murein synthesis, *Microb. Drug Resist. 2*, 155−157.
52. Vollmer, W., von Rechenberg, M., and Höltje, J.-V. (1999) Demonstration of molecular interactions between the murein polymerase PBP1B, the lytic transglycosylase MltA, and the scaffolding protein MipA of *Escherichia coli*, *J. Biol. Chem. 274*, 6726−6734.
53. Rather, P. N., Orosz, E., Shaw, K. J., Hare, R., and Miller, G. (1993) Characterization and transcriptional regulation of the 2′-N-acetyltransferase gene from *Providencia stuartii*, *J. Bacteriol. 175*, 6492−6498.
54. Connell, T. D., Black, W. J., Kawula, T. H., Barritt, D. S., Dempsey, J. A., Kverneland, K., Jr., Stephenson, A., Schepart, B. S., Murphy, G. L., and Cannon, J. G. (1988) Recombination among protein II genes of *Neisseria gonorrhoeae* generates new coding sequences and increases structural variability in the protein II family, *Mol. Microbiol. 2*, 227−236.
55. Cannon, J. G., Lee, T. J., Guymon, L. F., and Sparling, P. F. (1981) Genetics of serum resistance in *Neisseria gonorrhoeae*: the sac-1 genetic locus, *Infect. Immun. 32*, 547−552.
56. Lawson, F. S., Billowes, F. M., and Dillon, J. A. (1995) Organization of carbamoyl-phosphate synthase genes in *Neisseria gonorrhoeae* includes a large, variable intergenic sequence which is also present in other *Neisseria* species, *Microbiology 141*, 1183−1191.

BI051679S